Journal of Theoretical Biology 314 (2012) 1–9

Contents lists available at SciVerse ScienceDirect

Journal of Theoretical Biology

journal homepage: www.elsevier.com/locate/yjtbi

Stochastic cellular automata model of cell migration, proliferation and differentiation: Validation with *in vitro* cultures of muscle satellite cells

N. Garijo [a], R. Manzano [b], R. Osta [b], M.A. Perez [a,*]

[a] Multiscale in Mechanical and Biological Engineering (M2BE), Aragon Institute of Engineering Research (I3A), University of Zaragoza, María de Luna 3, 50015 Zaragoza, Spain
[b] LAGENBIO-Faculty of Veterinary, Aragon Institute of Engineering Research (I3A), University of Zaragoza, María de Luna 3, 50015 Zaragoza, Spain

HIGHLIGHTS

- A stochastic cellular automata model is proposed for adult muscle satellite cells.
- Proliferation, migration and differentiation are simulated.
- Proliferative capacity from physiological or pathological subjects are predicted.
- Cell distribution inside the culture well is also accurately simulated.
- Myotube formation is computed as typically occurs with adult muscle satellite cell.

ARTICLE INFO

Article history:
Received 20 March 2012
Received in revised form
10 June 2012
Accepted 2 August 2012
Available online 29 August 2012

Keywords:
Random-walk
Muscle satellite cells
Stochastic cellular automata model
Proliferation–migration–differentiation

ABSTRACT

Cell migration and proliferation has been modelled in the literature as a process similar to diffusion. However, using diffusion models to simulate the proliferation and migration of cells tends to create a homogeneous distribution in the cell density that does not correlate to empirical observations. In fact, the mechanism of cell dispersal is not diffusion. Cells disperse by crawling or proliferation, or are transported in a moving fluid. The use of cellular automata, particle models or cell-based models can overcome this limitation. This paper presents a stochastic cellular automata model to simulate the proliferation, migration and differentiation of cells. These processes are considered as completely stochastic as well as discrete. The model developed was applied to predict the behaviour of *in vitro* cell cultures performed with adult muscle satellite cells. Moreover, non homogeneous distribution of cells has been observed inside the culture well and, using the above mentioned stochastic cellular automata model, we have been able to predict this heterogeneous cell distribution and compute accurate quantitative results. Differentiation was also incorporated into the computational simulation. The results predicted the myotube formation that typically occurs with adult muscle satellite cells. In conclusion, we have shown how a stochastic cellular automata model can be implemented and is capable of reproducing the *in vitro* behaviour of adult muscle satellite cells.

1. Introduction

Cell migration and proliferation has been modelled as a process similar to diffusion in several works appearing in the literature (Lacroix et al., 2002). Bailón-Plaza and van der Meulen (2003) simulated cell migration as a diffusive process taking into account gradients in matrix density (haptotaxis). However, using diffusion models to simulate migration and proliferation tends to create a smooth variation in cell density that does not correspond to empirical observations. The use of stochastic (random-walk) or other models (cellular automata, particle models, *etc.*) (Turner and Sherrat, 2002; Börner et al., 2002; Alarcón et al., 2003; Longo et al., 2004; Simpson et al., 2007; Chopard et al., 2010) can overcome this limitation. Experiments demonstrating random movement of cells were done many years ago. For example, Ambrose (1961) observed the movement of an isolated fibroblast over the surface of a tissue culture dish as being mostly random, while Carter (1965) was among the first to demonstrate that cells execute a random walk on surfaces. More recently, Palsson and Bhatia (2004) observed, in an *in vivo* analysis, that a random spatial distribution could be produced during stem cell proliferation. Zohar et al. (1998) observed experimentally that mesenchymal stem cells (MSCs) disperse by crawling and convection in the fluid.

Continuum models can be used to model the response of biological systems (for example, individual cell's behaviour as migration, proliferation and differentiation and interaction among

* Corresponding author. Tel.: +34 976761000; fax: +34 976762670.
E-mail address: angeles@unizar.es (M.A. Perez).

0022-5193/$ - see front matter © 2012 Elsevier Ltd. All rights reserved.
http://dx.doi.org/10.1016/j.jtbi.2012.08.004

cells) at all levels from cells to tissue. Although key cell responses such as cell density evolution can be modelled using partial differential equations (PDEs), one important limitation of this method is that PDEs may not capture the discrete nature of multicellular biological systems consisting of individual cells and can become cumbersome when solving complex processes involving several variables (Hwang et al., 2009). Therefore, biological phenomena on the cellular level should use discrete methods; although population level dynamics are probably better modelled with other techniques. Different discrete methods have been mainly used for modelling multicellular biological systems: agent-based models (ABM) and cellular automata (CA), which is an ABM. In both, each individual cell is modelled based on behaviour rules defined specifically for it; likewise, the global system behaviour emerges through the local interactions among the cells based on the rules of behaviour at the cell level. The main difference between CA and ABM is that a lattice point must be defined for CA while ABM can be lattice free (Peirce et al., 2004; Simpson et al., 2007; Chopard et al., 2010; Landmann et al., 2011; Turner and Sherrat, 2002; Deutsch and Dormann, 2005; Drasdo and Höhme, 2005; Hatzikirou and Deutsch, 2008; Byrne and Drasdo, 2009; Hoffmann et al., 2011; Zahedmanesh and Lally, 2012). In this context, Alarcón et al. (2003) proposed an algorithm where the cells were considered as elements of a cellular automaton whose evolution rules were inspired by the different behaviour of normal and cancer cells; Longo et al. (2004) developed a CA computer model to analyse the spatial and temporal movements of blastocoel roof cells of the *Xenopus laevis* embryo during epiboly; and Peirce et al. (2004) developed a CA computational simulation that integrates epigenic stimuli, molecular signals, and cellular behaviour to predict microvascular network patterning events. Later, Simpson et al. (2007) used a CA algorithm which replicated travelling wavelike invasion profiles. Their approach allowed both the cell-scale and population-scale properties of invasion to be predicted in a way that was consistent with multiscale experimental data. More recently, Landmann et al. (2011) developed a CA simulation algorithm based on exclusion processes to test ideas for the emergence of the morphology of the enteric neural crest. Other studies introduced a lattice-gas cellular automaton (LGCA) model in a microscopic model of cell migration together with a mathematical tensor characterisation of different biological environments (Deutsch and Dormann, 2005; Hatzikirou and Deutsch, 2008). Hatzikirou and Deutsch (2008) used this system as a model of *in vivo* glioma cell invasion.

Most previous computer models studied the dynamics of neural crest cells (Simpson et al., 2007; Landmann et al., 2011), cancer cells (Alarcón et al., 2003) or mesenchymal stem cells (Hoffmann et al., 2011). However, no studies about adult muscle satellite cells have been performed. Adult muscle satellite cells are muscle committed progenitors located between the basal lamina and sarcolemma of the myofiber and necessary for muscle regeneration (Siegel et al., 2009). Under physiological conditions, these cells remain quiescent but maintain the ability to activate and proliferate after injury-derived stimuli. Once activated, satellite cells perform several rounds of proliferation and subsequently differentiate by elongating and fusing with each other or with the damaged myofiber to form the new multinucleated myotubes that will give rise to the regenerated myofibers (Hawke and Garry, 2001; Charge and Rudnicki, 2004).

In persuit of a better understanding of the role of the proliferation, migration and differentiation of adult muscle satellite cells on muscle regeneration under physiological and pathological conditions (amyotropic lateral sclerosis) a stochastic cellular automata model based on a random-walk approach to simulate the proliferation, migration and differentiation of cells (Pérez and Prendergast, 2007). We hypothesise that the three processes will be completely stochastic. The model developed aims to predict the behaviour of *in vitro* cell cultures with adult muscle satellite cells. For the model validation, *in vitro* growth and differentiation experiments have been performed with muscle satellite cells extracted from wild type (WT) and transgenic SOD1-G93A (TR) 7 day-old mice. Moreover, the cells were obtained from two postnatal muscle types: fast-twitch extensor digitorum longus (EDL) (FAST), with anaerobic metabolism, and low-twitch soleus (SOL) (SLOW), with aerobic metabolism (Manzano et al., 2011b). During the course of their experiments with satellite cell *in vitro* cultures, Manzano et al. in 2011 observed heterogeneus cell distribution inside the culture well (Manzano et al., 2011a).

2. Material and methods

2.1. Cell proliferation

The approach for modelling the proliferation of cells is based on the random-walk theory (Pérez and Prendergast, 2007). It is a stochastic process. Initially, in two dimensions, a cell is presumed to be surrounded by four locations that a daughter cell could occupy (Fig. 1). Lattice topology is square. During parent cell proliferation opposite "poles" are excluded (as shown in Fig. 1) because adjacent positions are far more likely to occur during mitosis. Cells can occupy neighbouring positions with equal probability p (see Fig. 1). Although Fig. 1 shows four free positions around the cell, in general this will not be the case because some positions may be already occupied. Therefore the model incorporates "contact inhibition of cell division" by checking for vacant positions while cells proliferate and depending on the available states (n), the probability value p is computed in order to fulfil the condition $\sum_{i=1}^{n} p_i = 1$. If all the surrounding positions are free, the probability p given in Fig. 1 will be equal to 1/4. If there is only one vacant position, the probability of being filled is equal to one. If all neighbouring positions are occupied, mitosis will not occur.

2.2. Cell migration (n_s, t_s)

Cell migration is also based on the random-walk theory (Pérez and Prendergast, 2007). Recognising that migration is a faster process than proliferation, a new location for a migrating cell is chosen several times during one iteration of the proliferation process (Siegel et al., 2009). In the stochastic cellular automata model proposed, migration is controlled by two parameters: n_s, the number of jumps that a cell performs during each proliferation iteration; and t_s, the jump size, *i.e.*, the distance that the cell covers in each jump. In the present simulations, five random jumps are considered for each cell during each iteration of the simulation ($n_s=5$ and $t_s=1$). At the end of the migration, the availability of that final position is checked. If that final position is

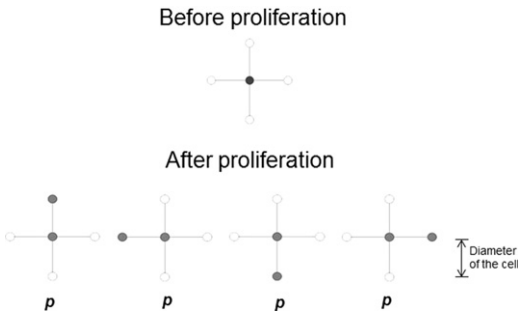

Fig. 1. Possible states that daughter cells can occupy after proliferation. The distance between the sites is only schematic; adjacent sites in the algorithm are considered to be exactly the diameter of a cell. p represents the probability for a daughter cell to be located in each proposed position (Lanza et al., 2005).

free, the probability of migrating to that point is one. If it is not free, the surrounding positions to the final one are checked following the same approach as for modelling the proliferation (Section 2.1). If the cell population is large enough to prevent migration (80% of the maximum total cell population allowed), then cells remain in their initial position without migration.

2.3. Cell differentiation

Cellular differentiation is the process by which a cell becomes a specialized cell type. As in the previous cases, differentiation is considered as a stochastic and discrete process. In the proposed model not all cells experience differentiation. The percentage of cells that differentiate has been assumed as p_d. From the population in the well, the cells which differentiate are chosen randomly and only those that have a neighbouring cell which they can join and begin to form a muscle cell are chosen. Subsequently, these cells are grouped with nearby cells, and they grow developing elongated structures similar to the experimentally observed myotubes.

These differentiated cells do not proliferate or migrate and can be considered as virtually immobile, their growth depending on the fusion of adjacent cells that will also become differentiated.

2.4. Numerical implementation

The stochastic cellular automata model has been developed on a circular lattice (6.34 mm in diameter) on the x–y plane (Fig. 2). The distance between the lattice points is 6.25 μm, assumed to be the value of the cell diameter (Lanza et al., 2005). The algorithm implementation is represented in Fig. 2. Each lattice site can only be occupied by one cell. The simulation starts with an initial population of 1000 cells randomly distributed in the cell culture. Cells start to proliferate following the process indicated in Section 2.1. The proliferation rate (p_r) indicates the percentage of the population that will divide. If the p_r value is inferior to 100%, proliferating cells are randomly selected among the whole population. In the light of the bibliography consulted (Manzano et al., 2011b; Pradat et al., 2011), two parameters have been considered to control the proliferation rate (p_r) in the present experimental conditions: p_1 represents the mouse genotype influence (WT *vs.* TR); p_2 defines the proliferation rate depending on the muscle type origin of the cells (FAST *vs.* SLOW). The combination of both parameters results in the proliferation rate p_r ($p_r = p_1.p_2$).

Once the cells have proliferated, migration is simulated using the random-walk theory. The migration process is assumed to be controlled by two parameters: the number of jumps (n_s) and the jump size (t_s), as described in Section 2.2.

After the 4.5th day of simulation, the algorithm introduces the differentiation process as described in Section 2.3. In this process, there is a percentage of cells that differentiates (p_d). As for the proliferation, it is assumed that the number of differentiating cells depends on the mouse genotype and muscle type origin. Cells that are going to differentiate are randomly chosen among the population, considering that cells that differentiate no longer proliferate nor migrate.

After differentiation, the cell positions are checked (check the collision—Fig. 2). If there are two cells in one position, one of the cells is removed (which would represent the death of the cell) and the number of collisions equals the number of cells removed.

Finally, the new population initiates a new iteration (one day of *in vitro* culturing) (Fig. 2).

The values assumed for these parameters are detailed in Table 1. The stochastic cellular automata model has been implemented in Matlab 7.10.0.

2.5. Model parameters

To summarise, the stochastic cellular automata model presented here has five model parameters: p_1, p_2 that control the proliferation rate (p_r) (see Section 2.1), n_s (number of jumps of a cell) and t_s (jump

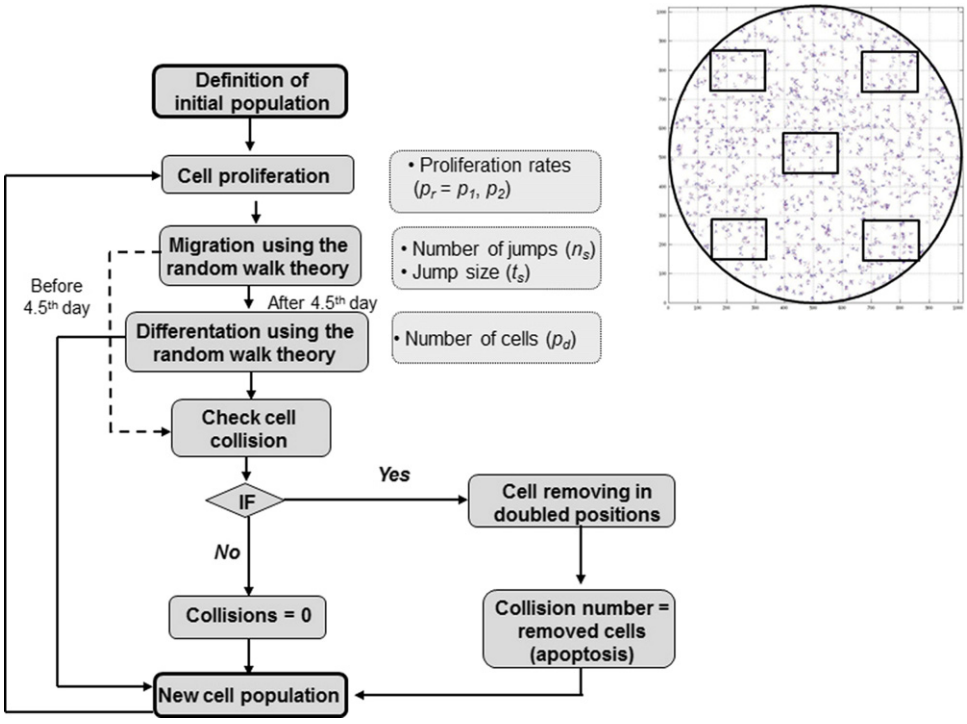

Fig. 2. Numerical implementation of the algorithm proposed and the circular well where the stochastic cellular automata model was implemented. The lateral and central regions where the experimental and computational measurements were done are indicated. The process is repeated iteratively, one iteration represents one day of *in vitro* culturing.

Table 1
Stochastic cellular automata model parameters.

Proliferation rates ($p_r = p_2 p_1$)			
	p_1 (%)		p_2 (%)
WT	100	FAST	100
TR	90	SLOW	60
Migration			
	n_s	t_s	
	5	1	
Differentiation rates (p_d)			
	WT-FAST	0.25	
	TR-FAST	0.18	
	WT-SLOW	0.07	
	TR-SLOW	0.05	

size) that control the migration process (Section 2.2) and p_d that defines the differentiation rate (Section 2.3). The determination of their values has been assumed to be phenomenological.

From the experimental results, it was observed that the proliferation behaviour was different depending on the mouse type and the muscle fibres from which the cells were extracted. FAST cells proliferated more than SLOW ones. There were also differences between the mouse types (WT *vs*. TR). The proliferation rate was lower in transgenic mice TR, and their proliferation rates were also more uniform during the whole experiment. Similar effects were observed with the differentiation patterns. FAST cells differentiated more than SLOW ones, and although small differences were observed between WT and TR from SLOW muscle fibres, a slightly higher differentiation was detected *in vitro* for the WT-SLOW than for the TR-SLOW cells. The differentiation rates (p_d) for each case (Table 1) were chosen following the differences observed experimentally. Therefore, the model parameters were defined according to previous experimental observations. Their values are represented in Table 1.

In order to validate the model, four different computational experiments were simulated considering the two types of mice and the two muscle origins: WT-FAST, TR-FAST, WT-SLOW and TR-SLOW. To obtain the computational results, 8 simulations of each case were performed. As the simulation is based on a stochastic model, it provides a different result each time. The cells were counted in four fields per simulation as in the experimental design. The four fields correspond to four lateral regions of the well. The size of the field considered for cell determination was 441×330 μm and corresponded to the experimentally used microscopic field (Fig. 2). Finally, the statistics of all the results were computed.

2.6. Experimental data

2.6.1. Adult muscle satellite cells

In vitro cell cultures of murine adult muscle satellite cells were used to validate the computational model. Transgenic mice with the G93A human SOD1 mutation (B6SJLTg[SOD1-G93A]1Gur) were purchased from The Jackson Laboratory (Bar Harbour, ME, USA). Hemizygotes were maintained by breeding SOD1-G93A males with wild type females. The offspring were genotyped by PCR amplification of DNA extracted from the tail tissue, as described in The Jackson Laboratory protocol for genotyping SOD1-G93A transgenic mice. All experimental procedures were approved by the Ethics Committee of the University of Zaragoza and followed the international and the institutional guidelines for the use of laboratory animals. Mice were housed under a 12 h light: 12 h dark cycle at 21–23 °C with relative humidity of 55%. Food and water were available *ad libitum*. The animals were sacrificed by cervical dislocation.

2.6.2. Satellite cell extraction and culture

Four WT and TR mice were sacrificed at a postnatal age of 7–10 days (p7). Typically fast-twitch EDL and slow-twitch SOL muscles were harvested and processed in parallel following the described protocol (Manzano et al., 2011b). Isolated cells were obtained by enzymatic tissue digestion and stained with 0.4% trypan blue (Sigma-Aldrich) for viable cell counting (Chakravarthy et al., 2000). Cultures were established with freshly isolated passage zero cells to avoid possible differences related to the susceptibility of WT and TR muscle satellite cells to freezing and trypsinization. For all the experiments, 96-well plates (6.34 mm diameter) coated with Matrigel basement membrane matrix (Becton Dickinson SA) were used and a total of 1000 cells per well were seeded. The culture medium was composed of 39% F-12+GlutaMAX (Gibco), 39% DMEM+GlutaMAX (Gibco), 10% fetal calf serum (Gibco) and 2% Ultroser G (Pall-Biosepra). The cells were left to adhere and start proliferating for 2.5 days at 37 °C and with 5% CO_2.

2.6.3. Cell proliferation assay

Starting 2.5 days after the plating and continuing until 7.5 days, the cell proliferation plates were daily fixed in 10% neutral buffered formalin solution (Sigma-Aldrich) and the nuclei were stained with Hoechst 33342 (Bis Benzimide H 33342 trihydrochloride, Sigma-Aldrich) for 5 min. For cell counting, the wells were washed with 1X PBS and four random fields (lateral regions—Fig. 2) per well were photographed under an epi-fluorescence microscope (Nikon TE2000-E) at 20× magnification and 325 nm. For each time point and group, the number of Hoechst positive nuclei of four replicate wells was counted (total 20 fields). A comparison of the experimental and the computational results is presented in the results section of the present paper.

2.6.4. Differentiation

The cell culture medium supported both proliferation and differentiation. Therefore, differentiation was progressively induced in the cell culture wells as populations reached the appropriate cell density. In order to monitor the satellite cell differentiation, a specific molecular marker for differentiating satellite cells, myogenin, was observed by immunohistochemistry. Moreover, the progressive formation of myotubes was daily checked in all the cell culture wells. Although no quantitative experimental results were obtained from the experimental data.

2.7. Statistical analysis

Experimental and computational data sets obtained from each group (WT-FAST, TR-FAST, WT-SLOW and TR-SLOW) were averaged for each day of culture, and a statistical analysis was performed for each timepoint by a comparison of both sets using the Student's *t*-test (Statistica 5.0, Statsoft software). Statistical differences were considered significant at $p < 0.05$.

3. Results

3.1. Cell proliferation percentage

No significant differences between the experimental and computational approaches were found for the proliferation curves obtained from daily satellite cell counting from 2.5 to 7.5 days of culture in any of the studied groups (WT-FAST, TR-FAST, WT-SLOW and TR-SLOW) (Fig. 3). The greatest differences between the experimental and computational results were found in the WT-SLOW group, especially during the last 3 days of culture, which could be explained by the increase in the standard error in the experimental approach. However, even in these cases, none of

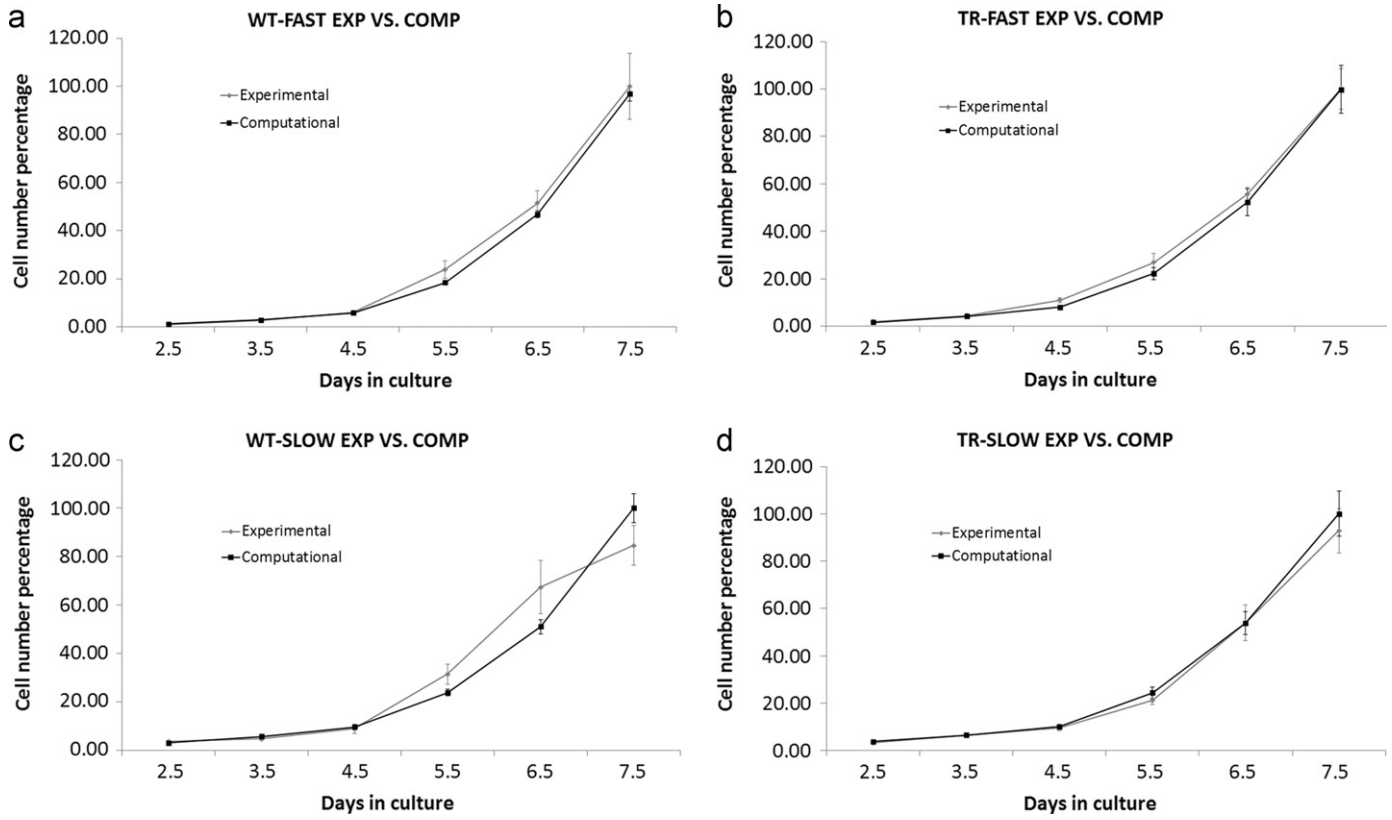

Fig. 3. Comparison of the experimental and computational cell proliferation capacity evolution for the cells extracted from: (a) WT-FAST; (b) TR-FAST; (c) WT-SLOW; (d) TR-SLOW. Row data were normalised setting the maximum value for each comparison to 100. Error bars represent the standard error of the mean as a percentage of the maximum value of the comparison set to 100.

the differences reached statistical significance. This validates the use of the present computational model to predict the proliferation ability of a given population. Moreover, two parameters influencing the proliferative dynamic of the satellite cells, phenotype and muscle type origin, were incorporated into the model in the light of the experimental results. Hence, the present model was capable of reproducing the proliferative capacity from physiological or pathological (neurodegenerative) subjects and from both muscle types.

3.2. Qualitative cell distribution in the well

During the first days of the experiments, it was observed that the cells were not homogeneously distributed across the surface of the well. There was a greater cell density distribution in the lateral area than in the centre (Fig. 4a). Therefore, cells were additionally counted in the centre of the well (experimentally and computationally) in order to compare the cell population in both regions (Fig. 2). The computationally obtained results predicted a similar trend to those obtained experimentally, the cell percentage being higher in the lateral area of the well than in the centre (Fig. 4b).

3.3. Sensitivity analysis of the migration parameters

The results shown in Figs. 3 and 4 were obtained using the following values for the migration parameters: the number of jumps equals 5 ($n_s=5$) and the jump size equals 1 ($t_s=1$). A sensitivity study of these parameters has been performed due to the lack of experimental information available (see Fig. 5).

It can be observed that increasing the number of jumps (n_s) resulted in an increase in the cellular percentage. There were also more cells when the jump size (t_s) increased. A combination of a high number of jumps and a high jump size increased the final cell population, but a more homogeneous distribution of cells in the well was predicted (Fig. 5a–f). A comparison among all the cases was represented in terms of cell percentage (Fig. 5g). The

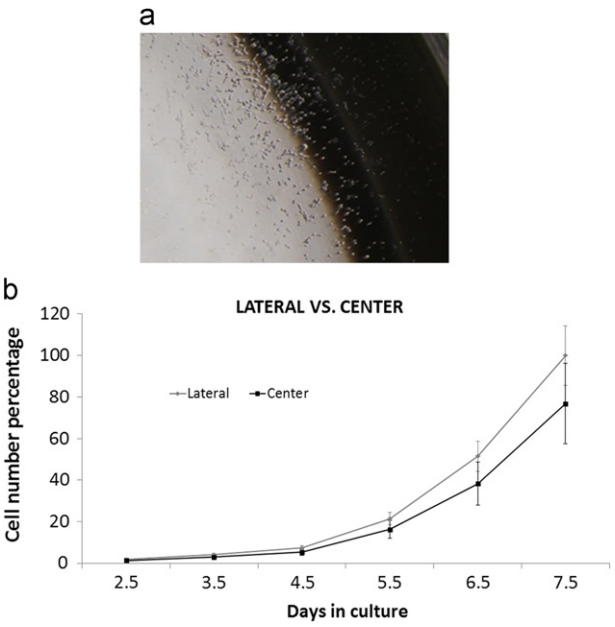

Fig. 4. (a) Details of the cell distribution in the lateral area of the culture well after the first days of culture obtained experimentally, (b) cell proliferation capacity predicted for the cells extracted from TR-FAST ($n_s=5$, $t_s=1$) in the lateral area and in the centre of the well.

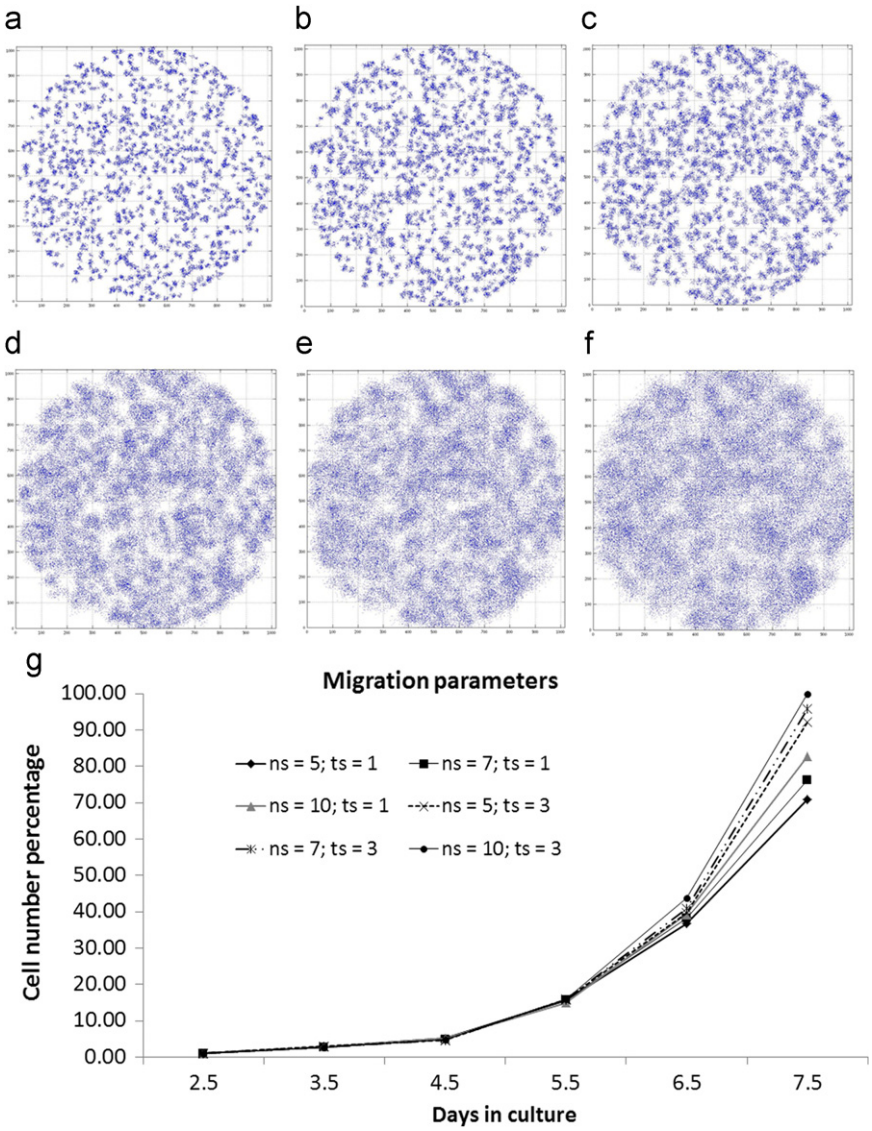

Fig. 5. Cell distribution predicted in the well for different migration parameters (n_s, t_s): (a) n_s=5, t_s=1; (b) n_s=7, t_s=1; (c) n_s=10, t_s=1; (d) n_s=5, t_s=3; (e) n_s=7, t_s=3; (f) n_s=10, t_s=3; (g) comparison of cell percentages obtained by incorporating different values of n_s and t_s to the simulation in TR-FAST cells. Row data were normalised setting the maximum value of all simulations to 100.

incorporation of contact inhibition of cell movement in the model was clearly demonstrated with this sensitivity analysis. When the parameters have low values, the cells migrate randomly around their original position. Therefore, there will be a lower number of free positions for the cells to proliferate in the next iteration and the number of cells that proliferate is reduced. When the parameters have higher values, the probability of having free positions surrounding the cells increases and the number of cells that proliferate also increase (Fig. 5).

3.3.1. *Differentiation patterns*

The results of the differentiation process are shown in Fig. 6. Experimentally, myogenin detection and subsequent myotube formation were evident in all groups (WT-FAST, TR-FAST, WT-SLOW and TR-SLOW) from day 4.5 of culture (Fig. 6a). This was therefore selected as the timepoint at which to incorporate the differentiation parameter into the model (see Fig. 2 and Section 2.4). The computational results show the progressive formation of elongated multicellular structures as the cells differentiate (Fig. 6b). A detailed image of these structures can be seen in Fig. 6c. The black arrows indicate the formation of elongated multinucleated structures reproducing the myotube formation. These structures resemble the myotube formation during the satellite cell differentiation in *in vitro* cultures and the ability of the present computational model to simulate the satellite cell differentiation process is therefore corroborated.

Differentiation patterns were also studied in the above mentioned sensitivity analysis of the migration parameters (data not shown). Increasing the jump size (t_s) did not produce the formation of elongated structures, as experimentally observed, but multinucleated circular structures were produced and the cells spread over the surface of the well, increasing their proliferations and filling the free positions. On the other hand, no significant differences were observed when modifying the number of jumps (n_s).

4. Discussion

The methodology presented in this work consists of a stochastic cellular automata model to simulate the behaviour of adult muscle satellite cells, including proliferation, migration and differentiation.

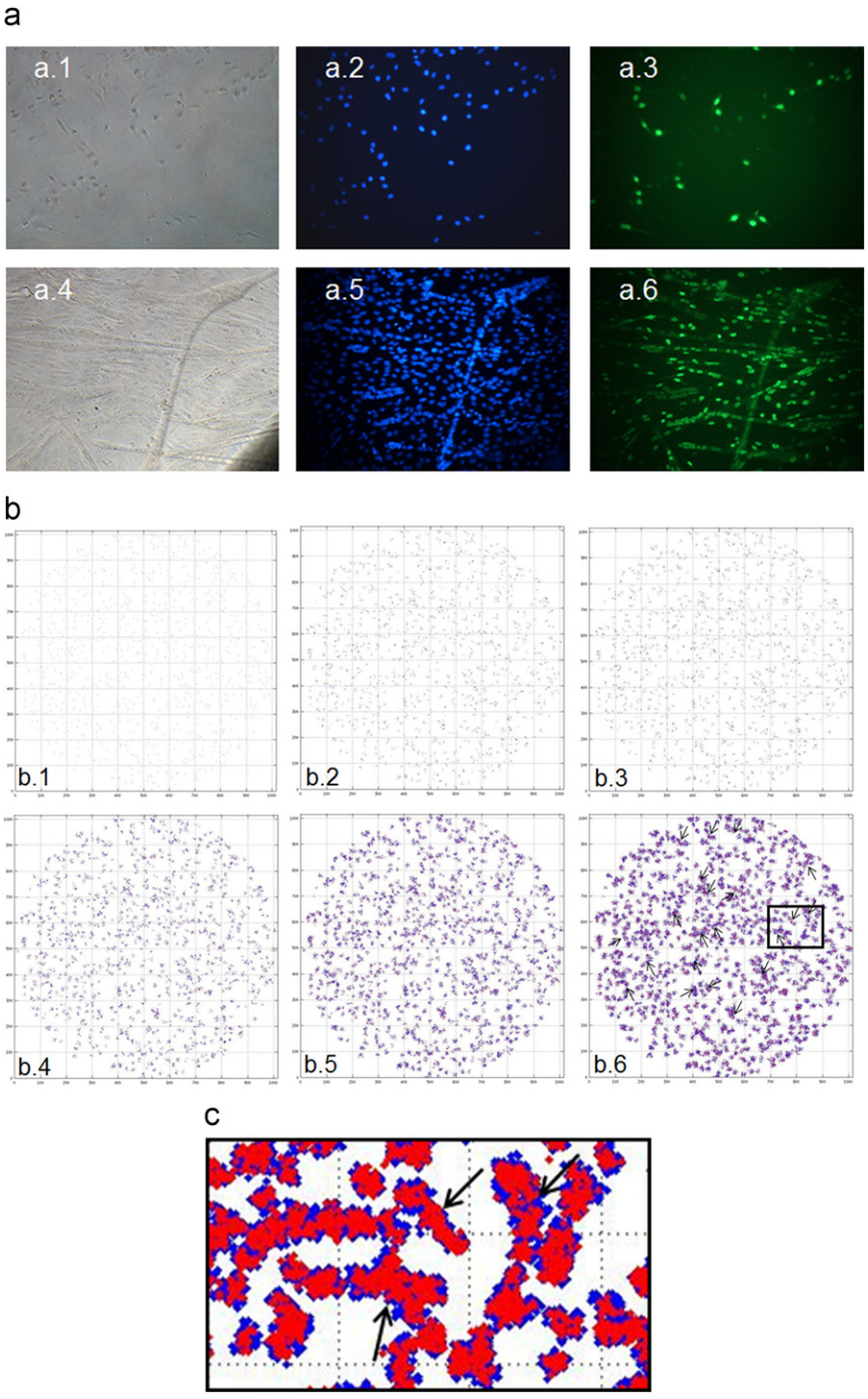

Fig. 6. Cell distribution during the differentiation process: (a) appearance of murine satellite cell cultures at 4.5 (a.1, a.2 and a.3) and 6.5 days (a.4, a.5 and a.6) postplating. a.1 and a.3 show bright field microscopy images; a.2 and a.4 show the Hoechst 33342 staining and a.3 and a.6 correspond to myogenin immunofluorescence analysis, respectively. Note the myogenin positive cell presence at 4.5 days of culture, and the increment in the proportion of these cells and the myotube formation as the differentiation progresses. (b) Representation of the computational results incorporating the differentiation parameter; differentiated cells are shown in red and undifferentiated cells in blue (b.1. 2.5 days; b.2 3.5 days; b.3 4.5 days; b.4 5.5 days; b.5 6.5 days and b.6 7.5 days). Black arrows indicate the formation of elongated multinucleated structures reproducing the myotube formation of the experimental cell culture. (c) Detail of the computational simulation of the differentiation process, obtained with TR-FAST cells and $n_s=5$, $t_s=1$ parameters. (For interpretation of the references to colour in this figure legend, the reader is referred to the web version of this article).

The model provides a mechanistic approach for this simulation. In the literature, several computer models have been developed to study the dynamics of different cell types such as neural crest cells (Simpson et al., 2007; Landmann et al., 2011), cancer cells (Alarcón et al., 2003) or mesenchymal stem cells (Hoffmann et al., 2011). However, to our knowledge, this is the first computational model dealing with adult muscle satellite cells.

The mechanism of cell dispersal is not diffusion. Cells disperse by crawling or proliferation, or are transported in a moving fluid. Discrete methods such as cellular automata or agent-based models can overcome this limitation (Chopard et al., 2010; Hoffmann et al., 2011). The proposed stochastic cellular automata model is based on previous discrete approaches. It depends on five parameters, mainly phenomenological: p_1 and p_2 control the

proliferation rate (p_r) and depend on the mouse genotype and the muscle type origin of the cells, respectively; n_s (number of jumps of a cell) and t_s (jump size) control the migration process and p_d defines the differentiation rate depending on the combination of mouse genotype and muscle type. Values assumed for p_1, p_2 and p_d were defined according to experimental observations (see Section 2.5), whereas for n_s and t_s a sensitivity analysis was performed in order to analyse their influence on proliferation, migration and differentiation.

The computational results paralleled those obtained with *in vitro* satellite cell cultures. Overall, no significant differences were found in the proliferation capacity predicted computationally and measured experimentally. Moreover, the main inputs influencing satellite cell proliferation *in vitro* such as mice genotype and muscle origin have also been considered in the present stochastic cellular automata model through the p_1, p_2 and p_d parameters. The results also support the view that satellite cells originating from SLOW and FAST muscles are intrinsically different as has been suggested for their proliferative ability (Manzano et al., 2011b) and regenerative potential (Kalhovde et al., 2005), and widely observed with mature skeletal muscle myotubes, which are known to differ into their enzymatic activities as well as metabolic and morphological properties (Zierath and Hawley, 2004; Patterson et al., 2006). These observations warrant further studies on the effect of cell origin for therapeutic approaches.

In addition, the present model proved capable of quantitatively reproducing the cell distribution in the well. Experimentally, cells tended to increase their density at the lateral sides of the well, and this tendency was corroborated by the stochastic cellular automata model.

In vitro, and under specific conditions of nutrients and cell density, muscle satellite cells elongate and fuse with each other to form nascent multinucleated syncitia myotubes, reproducing the events observed *in vivo* during postnatal growth and after muscle injury (Hawke and Garry, 2001; Charge and Rudnicki, 2004). This model is capable of reproducing these phenomena, and with the appropriate n_s values ($n_s=5$), the formation of elongated multicellular structures can be observed, as reported in the results section. On the other hand, in *in vitro* cultures it is known that proliferation and migration are properties limited to undifferentiated satellite cells (Hawke and Garry, 2001; Charge and Rudnicki, 2004). Consequently, the increment of n_s or t_s values, that would simulate an exacerbation of cell motility, is directly correlated to the proliferative ability of the cells (see Fig. 5g). In terms of cell differentiation, the increment of t_s values, a property of undifferentiated proliferating satellite cells, resulted in homogeneity in the cell distribution over the surface in the simulation approach, but not the formation of elongated structures that would correspond to myotube formation. This observation reinforces the accuracy of the computational results.

A limitation of the methodology proposed was that no quantitative information about the migration capacity of adult muscle satellite cells was found in the literature. Therefore, a sensitivity analysis of the two parameters controlling this migration (n_s and t_s) was done. Initially, a constant value for the parameters was assumed independently of the mice and muscle fibre type: the jump size (t_s) and the number of jumps (n_s) were assumed as 5 and 1, respectively. From our computational results, it was reported that they fundamentally affect the number of cells and the homogeneity of their distribution in the culture well. Nevertheless, it remains unclear to what extent cellular migration is involved in satellite cell-mediated regeneration. It seems plausible, however, that given the isolation and relatively sparse distribution of satellite cells in injured tissue, the accumulation of a large population of activated myoblasts at a site of focal injury would require directional motility. Early *in vivo* data is in agreement with the previous observation, suggesting that satellite cells may not only traverse the entire length of a myofibre but will also migrate between fibres (Bischoff and Heintz, 1994). Siegel et al. (2009) observed more persistent long-term contact between individual satellite cells than had been previously supposed, including potential cell-cell attractive and repulsive interactions and migration between host myofibres. Their data suggests that satellite cell migration *in vivo* may be more extensive than currently thought, and could be regulated by a combination of signals, including adhesive haptotaxis, soluble factors and guidance cues. Specific experiments should be performed in order to improve the migration parameter computation. Live microscopy will allow the estimation of these parameters (Henzé et al., 2011). Unfortunately, it is often difficult to relate the parameters of *in vitro* models to those of the stochastic cellular automata approach. Consequently, it is unclear if the behaviour observed in an *in vitro* experiment is the same as the behaviour that may be obtained from a large scale simulation using the stochastic cellular automata model for the same biological systems on a small scale.

Our experimental observations corroborated the results obtained from the computational stochastic cellular automata. The model developed can therefore be said to represent an interesting approach to reproducing the proliferation, migration and differentiation of *in vitro* skeletal muscle satellite cell cultures considering both the physiological and pathological variables that have been reported to influence the behaviour of these cells *in vivo* and *in vitro* (Manzano et al., 2011a). However, the influence of additional parameters such as gradients in biochemical factors, nutrients or oxygen have been described as determining the directional nature of motility *in vivo* in many cell types including satellite cells (Stokes and Lauffenburger, 1991; Terranova et al., 1985). Hence, we cannot rule out the possibility that subtle modifications of our results may arise from *in vivo* assays. Another limitation of the model was that cell size and shape have been considered to remain constant through the entire process, due to the evident difficulty of simulating the progressive generation of multinucleated sincitia where the size of the complex is modified by fusion of the cytoplasm of adjacent cells and the alignment of their nuclei. Lattice square topology was assumed in the present approach. This fact includes some artifacts as the pattern formation. There are other approaches as ABM which are lattice free, meaning that cells can be at any location in the computational domain as occurs experimentally. Additionally, hypothetic *in vitro* differences in myotube formation between both satellite cell origins are not feasible to be reproduced by the present computational model as they would derive from the above mentioned subcellular conditionants such as heterogenic enzymatic activities or mitochondrial content, not being these parameters considered in the model. These assumptions are necessary in order to simplify such a complex biological process. The accuracy of the model will improve as the number of assumptions incorporated in the design is reduced as a result of newly acquired experimentally-derived metrics. However, the computational nature of the stochastic cellular-automata model makes it highly accessible to further modifications, facilitates high throughput automated analysis, and rapidly generates useful data.

A stochastic cellular automata model for the simulation of cell proliferation, migration and differentiation (Pérez and Prendergast, 2007) has been used in combination with a mechanoregulation model in different mechanobiological problems including scaffold and tissue differentiation incorporating angiogenesis (Byrne et al., 2007; Khayyeri et al., 2009,2010,2011; Sandino et al., 2010; Checa and Prendergast, 2010) or the simulation of tissue formation in the lumen of an artery in response to the deployment of a stent (Boyle et al., 2010). Predictive tools relevant to these kinds of multiscale observations cannot be based on continuum or discrete models

alone. The ability to simulate processes occurring over a range of scales is required. In this context, the present model represents an interesting tool for depicting how individual cell interactions in a discrete model give rise to emergent population-scale patterns.

In conclusion, this is the first *in silico* model used to reproduce the behaviour of muscle satellite cells both under physiological and pathological conditions. The proposed stochastic cellular automata model enables the simulation of proliferation, migration and differentiation processes in adult muscle satellite cells. It can be easily implemented to simulate the performance of skeletal muscle stem cells and their capacity for repair and regeneration *in vitro*. These results may have special importance for regenerative medicine research into muscle or neuromuscular disorders (amyotropic lateral sclerosis), where the pool of muscle stem cells is often deplenished or disturbed. We consider this computational model to be a useful tool for many researchers working on muscle stem cell biology and the study of neurodegenerative diseases. It can serve as a methodology to simulate satellite cell dynamics depending on the variables included in each experimental design.

Acknowledgements

The authors gratefully acknowledge the research support of the Aragón Institute of Engineering Research (I3A) through its Multidisciplinary Research programme. The authors also gratefully acknowledge support from the Ministry of Science and Innovation through the projects PT-2009-0028, DPI2011-22413, PI10/0178 from the Fondo de Investigación Sanitaria of Spain and ALS association.

References

Alarcón, T., Byrne, H.M., Maini, P.K., 2003. A cellular automaton model for tumour growth in inhomogeneous environment. J. Theor. Biol. 225, 257–274.
Ambrose, E.J., 1961. The movements of fibrocytes. Exp. Cell Res. 8, 54–73.
Bailón-Plaza, A., van der Meulen, M.C.H., 2003. Beneficial effects of moderate, early loading and adverse effects of delayed or excessive loading on bone healing. J. Biomech. 36, 1069–1077.
Bischoff, R., Heintz, C., 1994. Enhancement of skeletal muscle regeneration. Dev. Dyn. 201, 41–54.
Börner, U., Deutsch, A., Reichenback, H., Bär, M., 2002. Rippling patterns in aggregates of myxobacteria arise from cell–cell collisions. Phys. Rev. Lett. 89 (7), 078101.
Boyle, C.J., Lennon., A.B., Early, M., Kelly, D.J., Lally, C., Prendergast, P.J., 2010. Computational simulation methodologies for mechanobiological modeling: a cell-centred approach to neointima development in stents. Philos. Trans. R. Soc. A 368, 2919–2935.
Byrne, D.P., Lacroix, D., Planell, J.A., Kelly, D.J., Prendergast, P.J., 2007. Simulation of tissue differentiation in a scaffold as a function of porosity, Young's modulus and dissolution rate: application of mechanobiological models in tissue engineering. Biomaterials 28, 5544–5554.
Byrne, H., Drasdo, D., 2009. Individual-based and continuum models of growing cell populations: a comparison. J. Math. Biol. 58, 657–687.
Carter, S.B., 1965. "Principles of cell motillity: the direction of cell movement and cancer invasion. Nature 208 (16), 1183–1187.
Charge, S.B., Rudnicki, M.A., 2004. Cellular and molecular regulation of muscle regeneration. Physiol. Rev. 84 (1), 209–238.
Chakravarthy, M.V., Davis, B.S., Booth, F.W., 2000. IGF-I restores satellite cell proliferative potential in immobilized old skeletal muscle. J. Appl. Physiol. 89 (4), 1365–1379.
Checa, S., Prendergast, P.J., 2010. Effect of cell seeding and mechanical loading on vascularisation and tissue formation inside a scaffold: a mechano-biological model using a lattice approach to simulate cell activity. J. Biomech. 43, 961–968.
Chopard, B., Ouared, R., Deutsch, A., Hatzikirou, H., Wolf-Gladrow, D., 2010. Lattice-gas cellular automaton models for biology: from fluids to cells. Acta Biotheor. 58 (4), 329–340.
Deutsch, A., Dormann, S., 2005. Cellular Automaton Modeling of Biological Pattern Formation. Birkhauser, Boston.
Drasdo, D., Höhme, S., 2005. A single-cell-based model of tumor growth *in vitro*: monolayers and spheroids. Phys. Biol. 2, 133–147.
Hatzikirou, H., Deutsch, A., 2008. Cellular automata as microscopic models of cell migration in heterogeneous environments. Curr. Top. Dev. Biol. 81, 401–434.
Hawke, T.J., Garry, D.J., 2001. Myogenic satellite cells: physiology to molecular biology. J. Appl. Physiol. 91 (2), 534–551.
Henzé, M.L., Collin, O., Terrier, E., Lennon-Doménil, A.M., Piel, M., 2011. Cell migration in confinement: microchannel-based assay. Methods Mol. Biol. 769, 415–434.
Hoffmann, M., Kuska, J.P., Zscharnack, M., Loeffler, M., Galle, J., 2011. Spatial organization of mesenchymal stem cells *in vitro*-results from a new individual cell-based model with podia. PLoS ONE 6 (7), e21960.
Hwang, M., Garbey, M., Berceli, S.A., Tran-Son-Tay, R., 2009. Rule-base simulation of multicellular biological systems—a review of modeling techniques. Cell. Mol. Bioeng. 2 (3), 285–294.
Kalhovde, J.M., Jerkovic, R., Sefland, I., Cordonnier, C., Calabria, E., Schiaffino, S., Lomo, T., 2005. "Fast" and "Slow" muscle fibres in hindlimb muscles of adult rats regenerate from intrinsically different satellite cells. J. Physiol. 562, 847–857.
Khayyeri, H., Checa, S., Tägil, M., Aspenberg, P., Prendergast, P.J., 2011. Variability observed in mechano-regulated *in vivo* tissue differentiation can be explained by variation in cell mechano-sensitivity. J. Biomech. 44, 1051–1058.
Khayyeri., H., Checa, S., Tägil, M., O'Brien, F.J., Prendergast, P.J, 2010. Tissue differentiation in an *in vivo* bioreactor: in silico investigations of scaffold stiffness. J. Mater. Sci. Mater. Med. 21, 2331–2336.
Khayyeri, H., Checa, S., Tägil, M., Prendergast, P.J., 2009. Corroboration of mechanobiological simulations of tissue differentiation in an *in vivo* bone chamber using a lattice-modeling approach. J. Orthop. Res. 27 (12), 1659–1666.
Lacroix, D., Prendergast, P.J., Li, G., Marsh, D., 2002. Biomechanical model to simulate tissue differentiation and bone regeneration application to frature healing. Med. Biol. Eng. Comput. 40, 14–21.
Landmann, K.A., Fernando, A.E., Zhang, D., Newgreen, D.F., 2011. Building stable chains with motile agents: insights into the morphology of enteric neural crest cell migration. J. Theor. Biol. 276 (1), 250–268.
Lanza, R., Thomas, E.D., Thomson, J., Pedersen, R., 2005. Essentials of Stem Cell Biology. Academic Press, New York.
Longo, D., Peirce, S.M., Skalak, T., Davidson, L., Marsden, M., Dzamba, B., DeSimone, D.W., 2004. Multicellular computer simulation of morphogenesis: blastocoel roof thinning and matrix assembly in *Xenopus laevis*. Dev. Biol. 271, 210–222.
Manzano, R., Toivonen, J.M., Calvo, A.C., Muñoz, M.J., Zaragoza, P., Osta, R., 2011a. Housekeeping gene expression in myogenic cell cultures from neurodegeneration and denervation animal models. Biochem. Biophys. Res. Commun. 407 (4), 758–763.
Manzano, R., Toivonen, J.M., Calvo, A.C., Miana-Mena, F.J., Zaragoza, P., Muñoz, M.J., Montarras, D., Osta, R., 2011b. Sex, Q1 fiber-type, and age dependent *in vitro* proliferation of mouse muscle satellite cells. J. Cell. Biochem. 112 (10), 2825–2836.
Palsson, B.O., Bhatia, S.N., 2004. Tissue Engineering, Pearson Prentice Hall Bioengineering, US.
Patterson, M.F., Stephenson, G.M.M., Stephenson, D.G., 2006. Denervation produces different single fiber phenotypes in fast- and slow-twitch hindlimb muscles of the rat. Am. J. Physiol. Cell Physiol. 291, 518–528.
Pradat, P.F., Barani, A., Wanschitz, J., Dubourg, O., Lombès, A., Bigot, A., Mouly, V., Bruneteau, G., Salachas, F., Lenglet, T., Meininger, V., Butler-Browne, G., 2011. Abnormalities of satellite cells function in amyotrophic lateral sclerosis. Amyotroph. Lateral Scler. 12 (4), 264–271.
Pérez, M.A., Prendergast, P.J., 2007. Random-walk models of cell dispersal included in mechanobiological simulations of tissue differentiation. J. Biomech. 40, 2244–2253.
Peirce, S.M., Van Gieson, E.J., Skalak, T.C., 2004. Multicellular simulation predicts microvascular patterning and in silico tissue assembly. FASEB J. 18 (6), 731–733, http://dx.doi.org/10.1096/fj.03-0933fje.
Sandino, C., Checa, S., Prendergast, P.J., Lacroix, D., 2010. Simulation of angiogenesis and cell differentiation in CaP scaffold subjected to compressive strains using a lattice modelling approach. Biomaterials 31, 2446–2452.
Siegel, A.L., Atchison, K., Fisher, K.E., Davis, G.D., Cornelison, D.D.V., 2009. 3D timelaspse analysis of muscle satellite cell motility. Stem Cell 27, 2527–2538.
Simpson, M.J., Merrifield, A., Landman, K.A., Hughes, B.D., 2007. Simulating invasion with cellular automata: connecting cell-scale and population-scale properties. Phys. Rev. E Stat. Nonlinear Soft Matter Phys. 76 (2 Pt 1), 021918.
Stokes, C.L., Lauffenburger, D.A., 1991. Migration of individual microvessel endothelial cells: stochastic model and parameter measurement. J. Cell Sci. 99, 419–430.
Terranova, V.P., Diflorio, R., Lyall, R.M., Hic, S., Friesel, R., Maciag, T., 1985. Human endothelial cells are chemotactic to endothelial cell growth factor and heparin. J. Cell Sci. 101, 2330–2334.
Turner, S., Sherrat, J.A., 2002. Intercellular adhesion and cancer invasion: a discrete simulation using the extended potts model. J. Theor. Biol. 216, 85–100.
Zahedmanesh, H., Lally, C., 2012. A multiscale mechanobiological modeling framework using agent-based models and finite element analysis: application to vascular tissue engineering. Biomech. Model. Mechanobiol. 11 (3–4), 363–377.
Zierath, J.R., Hawley, J.A., 2004. Skeletal muscle fiber type: influence on contractile and metabolic properties. PLoS Biol. 2 (10), e348.
Zohar, R., Cheifetz, S., McCulloch, C.A.G., Sodek, J., 1998. Analysis of intracellular osteopontin as a marker of osteoblastic cell differentiation and mesenchymal cell migration. Eur. J. Oral Sci. 106, 401–407.